ISIJ International, Vol. 56 (2016), No. 2, pp. 264–273

Calculation of Physical Properties for Use in Models of Continuous Casting Process-Part 1: Mould Slags

Kenneth C. MILLS,[1)]* Shyamprasad KARAGADDE,[2,3)] Peter David LEE,[2)] Lang YUAN[2,4)] and Fatemeh SHAHBAZIAN[5)]

1) Department of Materials, Imperial College, London, SW7 2AZ UK. 2) School of Materials, University of Manchester, Manchester, M13 9PL UK. 3) Department of Mechanical Engineering, Indian Institute of Technology Bombay, Mumbai, 400076 India. 4) GE Global Research, Nisakuyana, NY12309 USA.
5) KIMAB, SWEREA, Isafjordsgatan, 28A, 16440- Kista Sweden.

(*Received on July 3, 2015; accepted on September 3, 2015; J-STAGE Advance published date: January 14, 2016*)

Physical properties of both steels and mould slags are needed as input data for the mathematical modelling of the continuous casting process. Routines for calculating the properties of mould slags and for estimating steel properties have been developed and are described in Parts 1 and 2, respectively. Many mould powders, with differing compositions, are used in casting practice and their properties vary significantly. Reliable models have been developed to calculate these property values as a function of temperature from their chemical composition since this is available on a routine basis. Models have been developed to calculate the following properties: heat capacities, enthalpies, thermal expansion coefficient, density, viscosity, thermal conductivity and surface tension. Solid mould slags can exist as glassy or crystalline phases or as mixtures of the two (*i.e*. slag films) and the properties for the various phases can vary considerably; methods have been developed to calculate property values for these various states. The software used to calculate the properties is available via the link (i) http://www.mxif.manchester.ac.uk/resources/software (ii) https://sites.google.com/site/shyamkaragadde/software/thermophysical-properties.

KEY WORDS: mould slags; continuous casting; thermophysical properties; steels.

1. Introduction

Recent mathematical models[1–3)] have shown that that they are capable of providing (i) accurate predictions of both the heat flux and the powder consumption (a measure of the lubrication supplied to the shell) and (ii) valuable insights into the mechanisms underlying problems and defects (*e.g*. slag entrapment and oscillation mark formation). These models are being further developed to identify the causes of defects. However, models require accurate values for the physical properties of both the steel and mould slag (as input data). Properties of both mould slag and steel vary considerably with composition and a large number of steels and mould powders are in use. Consequently, a model of the continuous casting process requires a large amount of property data for the steel and mould powder used in the casting. The most satisfactory solution is to develop routines to calculate the required properties from their chemical composition, since the latter is available on a routine basis. The relationships developed to estimate the physical properties of mould slags from their chemical composition are described here in Part 1 and those used for steels are described in Part 2.The two models are linked to calculate the metal/slag interfacial tension.

Mould powders play an important role in the continuous casting process. They are added to the top of the mould and as they heat up the following events occur, sequentially (i) carbonates decompose to form CO_2(g) (ii) Carbon particles in the powder start to oxidise (iii) the oxide components sinter and (iv) then melt when the carbon is consumed, and molten globules mix to form a molten slag pool. Slag from the molten pool then infiltrates into the channel between the steel shell and the mould to form a slag film (**Fig. 1**); this consists of (i) a liquid layer (*ca.* 0.1 mm thick) and (ii) a solid layer (*ca.* 1–2 mm thick). The heat flux between shell and mould is determined, principally, by the thickness of this solid layer (and the amount of crystalline phase present) and the lubrication supplied to the shell is determined by the thickness of the liquid layer. Lubrication involves the following properties: viscosity (η), density (ρ) surface tension (γ) and break (or solidification) temperature (T_{br}). The heat flux involves the following properties of the mould slag: thermal conductivity (k), T_{br}, the fraction of crystalline phase formed in the slag film (f_{crys}) and the optical properties of the mould slag.

The objective of this study was to develop routines to provide reliable values of the thermo-physical properties of mould slags from their chemical compositions, for input into the model of the continuous casting process. The other aim was to make these routines available as Excel software; open access is provided at (i) http://www.mxif.manchester.ac.uk/resources/software (ii) https://sites.google.com/site/shyamkaragadde/software/thermophysical-properties.

1.1. Effect of Structure on Slag Properties

The properties of slags are principally determined by the structure of the slag. In silicate slags the basic building

* Corresponding author: E-mail: k.mills@imperial.ac.uk
DOI: http://dx.doi.org/10.2355/isijinternational.ISIJINT-2015-364

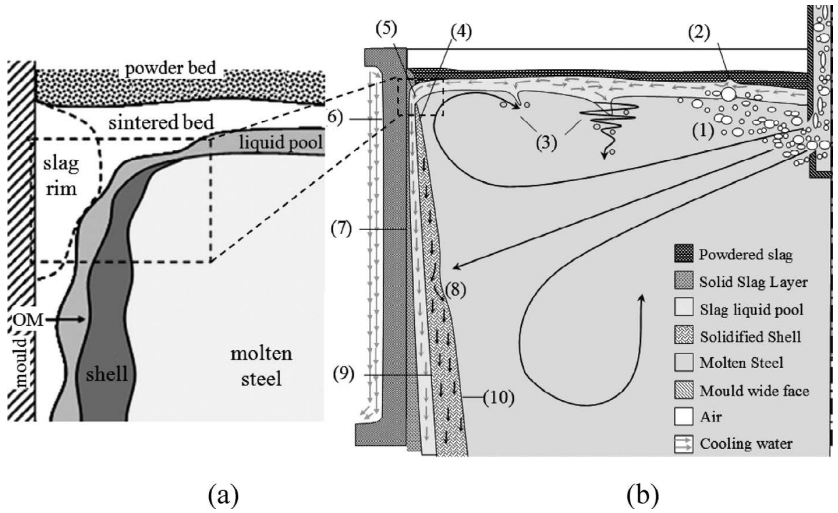

Fig. 1. Schematic drawings showings showing the various layers formed in the mould for (a) the meniscus area and (b) half-section of the mould.[1,3)]

block is the Si–O tetrahedron, in which one Si^{4+} cation is surrounded by 4 O^- ions. Furthermore, in pure silica, each of these O^- ions bonds to Si^{4+} ions in other tetrahedra to form a 3-dim. structure (these bonds are known as bridging O s (BOs)). When a cation, such as Na^+, is introduced into SiO_2, the Na^+ breaks the bridging O bond and forms a non-bridging O (NBO); this results in de-polymerisation of the slag. In highly-depolymerised slags some O ions are not bonded to Si ions, these are referred to as free oxygens (FOs).

In alumino- silicates, Al^{3+} ions are readily introduced into the Si^{4+} chain or ring but a Na^+ or 0.5 Ca^{2+} is needed for charge-balancing (*i.e.* to form $NaAl^{4+}$); cations on charge-balancing duties are not available for network-breaking. Thus the introduction of Al^{3+} ions result in an increase in the polymerisation of the slag, however, the Al–O bond is weaker than the Si–O bond.

Some properties, such as viscosity, electrical resistivity, diffusion coefficient and thermal conductivity are very dependent upon the degree of polymerisation. Several parameters have been used to represent the degree of polymerisation. In this paper the parameter, Q, is used; it can be calculated from Eqs. (1) and (2) where MO = CaO, MnO *etc.* and $M_2O = Na_2O$ *etc*. Summation index N_{MO} *etc.* represents the number of different oxides. Other properties, such as density, are affected by the structure but to a much smaller extent than that in the above properties.

$$\mathrm{NBO/T} = \frac{2\left(\sum_{1}^{N_{MO}} X_{MO} + \sum_{1}^{N_{M2O}} X_{M2O} - \sum_{1}^{N_{M2O3}} X_{M2O3}\right)}{\left(\sum_{1}^{N_{MO2}} X_{MO2} - 2\sum_{1}^{N_{M2O3}} X_{M2O3}\right)} \quad \text{..... (1)}$$

$$Q = 4 - \mathrm{NBO/T} \quad \text{..... (2)}$$

The O^- ions bonded to cations tend to be arranged into an octahedral array (*i.e.* they have 6- fold coordination) but this varies with cation size.[4)] In general, the effect of different cations on the physical properties is much smaller than the effect of polymerisation. Nevertheless, the nature of the cations affects both the structure and the physical properties. The parameter usually used to represent the effect of cations is the *field strength* ($=z/r^2$ where z and r are the charge and radius of the cation). Increasing field strength has been reported to bring about (i) a wider spread of polymerised silicate anions (*i.e.* a wider spread of Q^n species) (ii) a decrease in coordination number which affects the concentrations of BOs and NBOs (iii) increasing disorder in the melt or glass and (iv) a lower probability that they will carry out charge- balancing duties (which are usually carried out in the hierarchy $K^+ > Na^+ > Li^+ \approx Ba^{2+}$ *etc*). Cations affect properties (i) *directly* or (ii) *indirectly* through their effect on the structure; two examples of direct effects are (a) the electrical conductivities (κ) and diffusion coefficients (D) are affected by the number of available cations and for $X_{Na2O} = X_{CaO}$ there are twice as many Na^+ ions as Ca^{2+} cations (so $\kappa_{Na2O\ slag} > \kappa_{CaO\ slag}$ and $D_{Na2O\ slag} > D_{CaO\ slag}$) and (b) the *mixed alkali effect* occurs where some properties for slags are significantly affected by cations with differing size (*e.g.* K^+ and Li^+).

Increasing temperature has a similar effect to that of increasing the number of cations, *i.e.* it reduces the degree of polymerisation; thus increasing temperature reduces viscosity and increases electrical conductivity and diffusion rates.

1.2. Crystalline, Glassy and Liquid Phases

In the solid state, slags can exist as crystalline or glassy phases or as a mixture of the two phases (*e.g.* slag film). In *crystalline solids*, the ions occupy regular positions and the amount of disorder (or configurational entropy) is low. In contrast, *in glasses* the ions are more disordered and the configurational entropy is much higher than that in crystals.

The formation of glasses is promoted by (i) slags with high Q (degree of polymerisation) values (*i.e.* high SiO_2 contents) and (ii) fast cooling rates. When a frozen glass is heated, it transforms at the *glass transition temperature* (T_g) into a supercooled liquid (*scl*). This transition is accompanied by step-increases in both C_p and thermal expansion coefficient (α) and results in a concomitant increase in configurational entropy.

When a liquid slag is cooled, if crystals are precipitated, there is a sharp increase in viscosity at a certain temperature, often denoted as the *break temperature* (T_{br}). In contrast, if a *scl* is formed the viscosity increases smoothly with decreasing temperature.

2. Model Details

2.1. Composition, Modelling Parameters

The mould slag compositions covered by the model include conventional F- containing powders and F- free powders but do not include, at this time, the mould slags (based on calcium aluminates) now being used to cast

high- Al, high- Mn steels. Furthermore, B_2O_3 additions have been reported to both reduce and increase slag viscosities of mould slags by various investigators; for this reason the effect of B_2O_3 on viscosity has been excluded.

As –received, casting powders contain both free carbon and carbonate; these constituents are lost on ignition (LOI) in the process of forming a casting slag. The fraction of powder forming slag (f*) can be calculated from the chemical composition using either Eqs. (3) or (4)

$$f^* = (100 - \%LOI)/100 \quad \text{..... (3)}$$

$$f^* = (100 - \%C_{free} - (44/12)(\%C_{total} - \%C_{free}) \quad \text{..... (4)}$$

The composition of the casting slag can then be calculated by (i) multiplying by (1/f*) and normalising the composition. The software (covering these models) has the option to take into account typical pick-up values for Al_2O_3, FeO and MnO during casting. If this option is used the slag composition is re-normalised.

Mole fractions (X) are then calculated from these normalised compositions using Eq. (5) (where i refers to the constituents *e.g.* CaO, SiO_2 *etc.*); the %F present is converted into X_{CaF2} and the Ca^{2+} associated with the F^- ions is deducted from X_{CaO}.

$$X_i = (X_i / M_i)/\Sigma(X_i / M_i) \quad \text{..... (5)}$$

The ***mean molecular weight*** (M) is calculated using Eq. (6)

$$M = \Sigma(X_i M_i) \quad \text{..... (6)}$$

The ***parameter (NBO/T)*** is used as a measure of the depolymerisation of the slag. It is calculated from Eq. (1) where $\Sigma X_{MO} = X_{CaO} + X_{MgO} + X_{FeO}$ *etc.* and $\Sigma X_{M2O} = X_{Na2O} + X_{K2O}$ *etc.* The parameter, Q is a measure of the polymerisation of the slag and is calculated from (NBO/T) using Eq. (2). It should be noted that both X_{CaF2} and X_{TiO2} are ignored in Eq. (5) (on the basis of structural evidence) and the calculated Q value is that of the remaining slag (Q^{rem}).

The ***fraction of crystalline phase in the slag film*** (f_{crys}) was calculated using the relation proposed by Li *et al.*[5] where (NBO/T)* indicates that the parameter differs from that calculated with Eq. (1), in that (i) CaF_2 is included in network breakers and (ii) when %MgO and %MnO are >7% and >4%, respectively, they are included in the denominator of Eq. (1).

$$f_{crys} = -2.84 + 1.41(NBO/T)^* \quad \text{..... (7)}$$

$$\%_{crys} = 100.\ f_{crys} \quad \text{..... (8)}$$

2.2. Temperatures (T_g, T_{crit}, T_{liq} and T_{br})

These temperatures are calculated from chemical composition by the software and the temperature scale in the program is adjusted automatically.

The ***glass transition temperature*** (T_g) is the temperature where, on heating, a frozen glass transforms into a super-cooled liquid (*scl*). This transition is accompanied by step-increases in C_p and thermal expansion coefficient (TEC) (*i.e.* $3\alpha < T_g \approx \alpha > T_g$). The viscosity of a glassy slag is taken to have a value of $10^{13.4}$ (d Pas) at T_g (*i.e.* $\log_{10}\eta$ (d Pas)=13.4)).

Numerical analysis of a database of T_g values (840–910 K) obtained from C_p and TEC data[6] and chemical composition data for 23 mould slags was carried out in this study. Inspection of T_g values for mould slags indicates that values of mould slags tend to have similar values (T_g=870±30 K). The best fit results are shown in Eq. (9) and are used in the software. The uncertainty in the calculation is *ca.* ±20 K.

$$T_g(K) = 906 - 330.5X_{SiO2} + 190X_{CaO} + 440X_{Al2O3} - 449X_{N2O+K2O} - 11X_{MgO} + 154X_{CaF2} - 309X_{MnO} - 1391X_{FeO} \quad \text{..... (9)}$$

The ***critical*** **(*or deformation*)** ***temperature*** (T_{crit}) is the temperature, above which, the thermal conductivity, decreases rapidly with increasing temperature (this can be seen in **Fig. 6**). Thermal conductivity- viscosity plots reveal that T_{crit} occurs when $\log_{10}\eta$ T_{crit} (dPas)=6 *i.e.* between the *softening* and *flow* temperatures.[7] Values of the thermal conductivity as a function of temperature for a number of mould slags indicate that T_{crit} occurs at 1 040±10 K.[8,9]

The liquidus temperature (T_{liq}) is the temperature where the slag becomes fully molten. A numerical analysis of T_{liq} values (from DSC experiments) and composition data gave Eq. (10); the calculated values are subject to uncertainties of ±30 K.

$$T_{liq}(K) = 1464 - +11.4\%SiO2 - 11\%CaO + 4.2\%Al_2O_3 + 5.7\%MgO - 10.1\%Na2O - 15.8\%K_2O + 10\%Li_2O + 1.9\%F + 8.3\%FeO + 11.6\%MnO \quad \text{.. (10)}$$

More recently, numerical analysis was carried out on a database of T_{liq} and chemical composition data for 23 mould slags[6] and the Eq. (11) was obtained and is preferred. Values are subject to uncertainties of ±25 K.

$$T_{liq}(K) = 1473 - 1.518\%SiO_2 + 2.59\%CaO + 1.56\%Al_2O_3 - 17.1\%MgO - 9.06\%Na_2O - 6.0\%K_2O + 18\%Li_2O + 4.8\%\ F - 9.87\%FeO - 2.12\%MnO \quad \text{..... (11)}$$

The ***solidification temperature*** (T_{sol}) is the temperature where solids are first precipitated on cooling. It is frequently represented by the ***break temperature*** (T_{br}) which is the temperature below which the viscosity shows a sharp increase in viscosity during cooling. The break temperature decreases with increasing cooling rate and often T_{br} is cited for a cooling rate of 10 $Kmin^{-1}$. The thickness of the solid slag layer (Fig. 1) is partially- determined by the break temperature. The following equation was obtained from numerical analysis of T_{br} and chemical composition data;[10] these values are subject to uncertainties of ±30 K.

$$T_{br}(K) = 1393 - 3.3\%SiO_2 + 8.65\%CaO - 8.45\%Al_2O_3 - 17.1\%MgO - 3.2\%Na_2O - 2.2\%K_2O - 6.6\%Li_2O - 6.47\%\ F - 18.4\%FeO - 3.2\%MnO \quad \text{..... (12)}$$

In general, super-cooling will ensure that $T_{br} < T_{liq}$. However, the calculation of both T_{br} and T_{liq} involve an uncertainty of ±25–30 K, so cases where $T_{liq} < T_{br}$ do occur occasionally; in these cases a warning is issued on the Collected Worksheet.

2.3. Heat Capacity (C_p) Enthalpy ($H_T - H_{298}$)

The C_p- T relationships are different for different phases. Consequently, the mould slags are first sorted into individual phases *i.e.* (i) crystalline (b) glass (iii) slag film and (iv) liquid. The C_p and enthalpy of mould slags are little affected by the slag structure and it has been shown[11,6] that they can be calculated using routines based on partial molar quantities

$$P = \sum_{i=1}^{N}(X_i P_i) \quad \text{..... (13)}$$

where P is a property, or coefficient, X is the mole fraction

Table 1. The coefficients used in the calculation of C_p for crystalline phase C_p ($JK^{-1}mol^{-1}$) = $a^*+b^*T-c^*/T^2$; C_p for liquids ($JK^{-1}mol^{-1}$): and ΔS^{fus}: ($JK^{-1}mol^{-1}$).

	SiO_2	CaO	Al_2O_3	MgO	Na_2O	K_2O	Li_2O	FeO	MnO	CaF_2	ZrO_2	TiO_2	B_2O_3
a*	56.0	48.8	115	42.7	65.7	65.7	65.7	49	46.4	59.8	69.6	75.2	
10^3b*	15.4	4.52	11.8	7.45	22.6	22.6	22.6	8.37	8.1	30.45	7.53	1.17	
10^{-5}c*	14.4	6.53	35.1	6.2	0	0	0	2.8	3.88	−1.97	14.1	18.2	
C_p(l)	87	90.8	146.4	90.4	92.1	74.1	96.2	76.6	79.9	96.2	113	111.7	
ΔS^{fus}	4.6	24.7	50.2	24.7	33.9	33.9	33.9	9.6	18.8	18	25.1	26.8	

and i=1,2,3,…N denotes the different components (*e.g.* CaO, SiO_2 *etc.*).The values of C_p and (H_T-H_{298}) are calculated in units of $JK^{-1}mol^{-1}$ and $kJK^{-1}\ kg^{-1}$, respectively; values were converted from mol^{-1} to kg^{-1} by multiplying by (1 000/M) where M, the average molecular weight of the slag.

The temperature dependence of C_p for *crystalline solids* is usually expressed in the form:

$$C_p = a^* + b^* T - c^*/T^2. \quad \text{..... (14)}$$

where a*, b* and c* are constants (given in **Table 1**). In the model the parameters "a*" "b*" and "c*" are treated as partial molar quantities:[10] *e.g.*

$$a^* = \sum_{i=1}^{N} \left(X_i a^*_i \right) \quad \text{..... (15)}$$

The parameters b* and c* are calculated in a similar manner to a*.

The enthalpy (H_T-H_{298}) is given by:

$$\left(H_T - H_{298}\right) = \int_{298}^{T} C_p dT = a^*\left(T-298\right) + 0.5b^*\left(T^2 - 298^2\right) + \left(c^*/T\right) - \left(c^*/298\right) \quad \text{..... (16)}$$

The enthalpy of fusion, ΔH^{fus}, is calculated by assuming the entropy of fusion (ΔS^{fus}) can also be calculated from partial molar terms.

$$\Delta S^{fus} = \sum_{i=1}^{N} \left(X_i \, \Delta S_i^{fus} \right) \quad \text{..... (17)}$$

$$\Delta H^{fus} = T_{liq} \Delta S^{fus} \quad \text{..... (18)}$$

The C_p for the ***liquid phase*** is also calculated from partial molar terms[11] using Eq. (19) and the enthalpy for the liquid is determined from Eq. (20).

$$C_p = \sum_{i=1}^{N} \left(X_i \, C_{pi} \right) \quad \text{..... (19)}$$

$$\left(H_T - H_{298}\right) = \left(H_{Tliq} - H_{298}\right)_{sol} + \Delta H^{fus} + C_{p\ liq}\left(T - T_{liq}\right) \quad \text{.... (20)}$$

The C_p for the glass phase is close to that of the crystalline phase for temperatures below T_g. At T_g the frozen glass transforms to a ***super-cooled liquid*** (*scl*); this is accompanied by a step- increase in C_p. Measured values of C_p for the *scl* ($C_{p\ scl}$) were between 1 400 and 1 500 $JK^{-1}kg^{-1}$.[6,12] These values are in close agreement with the value calculated for the liquid.

Consequently it was assumed that $C_{p\ scl} = C_{p\ liq}$ for the range between T_g and T_{liq}. Values of the enthalpy for the *scl* in the temperature range between T_g and T_{liq} are given in Eq. (21).

$$\left(H_T - H_{298}\right)_{scl} = \left(H_{Tg} - H_{298}\right) + C_{p\,scl}\left(T - T_g\right) \quad \text{.... (21)}$$

It should be noted that:

(i) Crystallisation occurs around 50–100 K above T_g (this is an exothermic reaction and results in an *apparent* decrease in C_p in DSC measurements); thus the state of the sample remains largely undefined in this temperature range.

(ii) When ($H_{Tliq}-H_{298}$) is calculated for both crystalline and *scl* it was found that $(H_{Tliq}-H_{298})_{cryst} > (H_{Tliq}-H_{298})_{scl}$ which suggests that $\Delta H^{fus} \neq 0$ for the *scl*; high temperature C_p measurements are needed to resolve this anomaly.

The ***slag film*** consists of a mixture of glass and crystalline phases; the C_p and enthalpy for a slag film is calculated using the rule of mixtures (Eqs. (22) and (23), respectively).

$$C_{p\ slag\ film} = f_{cryst} C_{p\ \ cryst} + \left(1 - f_{cryst}\right) C_{p\ gl} \quad \text{..... (22)}$$

$$\left(H_T - H_{298}\right)_{slag\ film} = f_{cryst}\left(H_T - H_{298}\right)_{cryst} + \left(1 - f_{cryst}\right)\left(H_T - H_{298}\right)_{gl}. \quad \text{.... (23)}$$

There are only a few measurements of the C_p and (H_T-H_{298}) available for mould slags[6,12] and these are restricted to temperatures below 1 000 K. there are no reported measurements for the liquid. Thus the model is based on a generic data for oxides and fluorides. Although, the predicted C_p and (H_T-H_{298}) values are within ±2% of the experimental values for T < 1 000 K, the uncertainty is probably ±5% for T > 1 000 K. It should also be noted that when a glass is heated to a temperature of *ca.* (T_g +80 K) the sample will partially crystallise and the exothermic enthalpy released causes a sudden *apparent* decrease in C_p values measured by DSC; this is not a true effect and the values calculated by the model will not show this effect.

2.4. Density (ρ) Thermal Expansion Coefficient (α)

Thermal expansion coefficients reported for 10 glassy samples over the temperature ($298-T_g$) range between 9 and $11\times10^{-6}\ K^{-1}$ and for one sintered mould flux (298–1 100 K).[6] These measurements indicated that α decreased slightly with increasing Q ($10^6\ \alpha = 15.2–2.14\ Q$) but the scatter was such ($R^2 = 0.41$) that a constant value of $\alpha = 10\times10^{-6}\ K^{-1}$ has been preferred in the calculations. There are few data available for partially-crystallised samples of mould slag; one sample[6] exhibited a value of α(298–1 100 K) = $10\times10^{-6}\ K^{-1}$; this value was adopted.

The ***thermal expansion coefficient data*** for binary silicates in the liquid indicate that it is dependent upon both Q and (z/r^2).[13] However, there are few reported ρ- T data for liquid mould slags and individual ρ values are subject to uncertainty. Consequently, thermal expansion values for the liquid phase were obtained with a generic model for oxide slags[11] containing CaF_2.

The ***densities*** of silicate and alumino-silicate slags exhibit only a small dependence on the slag structure. Reasonable estimates can be obtained using partial molar volumes (V) for the various slag constituents but special procedures are

needed for SiO_2 and Al_2O_3.[11]

There are few reported data for the density of mould slags. Values have been reported for the glassy phase[14–16] the liquid state[17,18] and for some slag films.[12]

The density of the liquid mould slag is calculated from partial molar volumes ($V = M/\rho$ where M = molecular weight) as shown in Eqs. (24)–(26) (using the data given in **Table 2**) but special treatment is given to SiO_2 ($V_{SiO2} = 19.55 + 7.966X_{SiO2}$) and Al_2O_3 ($V_{Al2O3} = 28.31 + 32X_{Al2O3} + 31.45 (X_{Al2O3})^2$) to account for the effect of structure on the molar volume and hence the density (ρ).[11] These routines were calculated from studies of density values for a wide range of slag compositions.[11]

$$V_{l\,773} = \sum_{i=1}^{N} (X_i V_i) \quad \text{..... (24)}$$

$$V_T = V_{l\,773} + 0.01(T - 1\,773\ K) \quad \text{..... (25)}$$

$$V_T = M / \rho_T \quad \text{..... (26)}$$

Stebbins *et al.*[19] have also reported values of $V_{l\,873}$ and dV/dT based on regressions of V-T and (dV/dT) data for most of the components shown in Table 2. These data were used to calculate both $V_{l\,873\,K}$ and (dV/dT). Values for the missing components in Table 2 were derived here from ρ-T and V-T data.

The recommended values of V_T were calculated using the $V_{l\,773}$ value and Eq. (27) and are preferred to values calculated by Eq. (25). The values calculated using the Stebbins value for $V_{l\,873}$ are given on the Density Worksheet. Although V_T values in Table 2 vary, the density values calculated with the Stebbins parameters lie within 1% of those calculated by Eq. (27).

$$V_T = \Sigma X_i V_{l\,773} + \Sigma X_i (dV/dT)(T - 1\,773\ K) \quad \text{.... (27)}$$

A similar approach to that used for the liquid is taken for solid phase with different values for the molar volume (Table 2) and ($V_{SiO2} = 23.76 + 3.5X_{SiO2}$) and ($V_{Al2O3} = 40.4$). However, when a glassy sample crystallises it is accompanied by shrinkage (since $\rho_{crys} > \rho_{gl}$). This results in porosity in the sample; the porosity levels were not determined for the density measurements on slag films[12] but would be expected to lower the density values.

There are very few data reported for mould slags. The glassy phase has a lower density than the crystalline phase but there are no experimental data for mould slags to validate this statement. Thus, it has been assumed that $\rho_{gl} = \rho_{crys.}$ for temperatures between T_g and T_{liq}; the density of the super-cooled liquid was calculated by assuming that (i) there was no density change associated with the (*scl* → liquid) transition (ii) ρ_{scl} is a linear function over this temperature range (*i.e.* $\rho_T = \rho_{Tg} + (T - T_g)(\rho_{Tliq} - \rho_{Tg})/(T_{liq} - T_g)$.

Values of ρ_T for solids (both the glassy and sintered samples) were calculated using a value of $\alpha = 10^{-5}\ K^{-1}$. Normally, the calculations produce a density decrease at T_{liq} but the uncertainty in the calculations of ρ_T for both solid and liquid phases can lead (with certain compositions) to an apparent increase in density at T_{liq}; this is not a true effect and is caused by the combined uncertainties. In such circumstances a warning is given on the Collected Worksheet.

There are few reported density data for mould slags. Nevertheless, the estimated values for the density for temperatures below 1 000 K, the uncertainties are probably 2–3% and are within ±5% for T > 1 000 K. Data are needed for the density change associated with glass→ crystalline phase change.

2.5. Viscosity (η)

The principal factor affecting the viscosities of slags is the degree of polymerisation present in the slag; this can be clearly seen in **Fig. 2** where both $\ln \eta_{l\,900\,K}$ and the parameter, B_η exhibit considerable sensitivity to the parameter, Q (which is a measure of the polymerisation). The scatter of individual points in Fig. 2(a) is due to the effect of different

Table 2. Partial molar volumes (V_{1773}) used in the calculation of the density of the liquid; a denotes for $V_{SiO2} = 19.55 + 7.966X_{SiO2}$) b for Al_2O_3 ($V_{Al2O3} = 28.31 + 32X_{Al2O3} + 31.45 (X_{Al2O3})^2$) and V_{298} for the solid; c for SiO_2, $V_{SiO2} = 23.76 + 3.5X_{SiO2}$.; V_{1873} and (dV/dT) in the 4th and fifth row are from Stebbins[21]; * indicates calculated here.

	SiO_2	CaO	Al_2O_3	MgO	Na_2O	K_2O	Li_2O	FeO	MnO	CaF_2	ZrO_2	TiO_2	B_2O_3
$V_{1\,773}$(l)[11]	a	20.7	b	16.1	33	51.8	16	15.8	15.6	31.3		24	10
V_{298}	c	14.4	40.4	12.5	20.2	33.5	11	16.5	17	28.5	–	–	–
$V_{1\,673}$ *[21]	26.75	16.9	37.7	11.95	29.5	48.5	17.7*	13.7	13.3*	31*		24.25	27*
10^3dV/dT[21]	−0.42	3.97	1.02	2.22	7.4	2	1.5*	4.15	4*	5.1*		0.8	4*

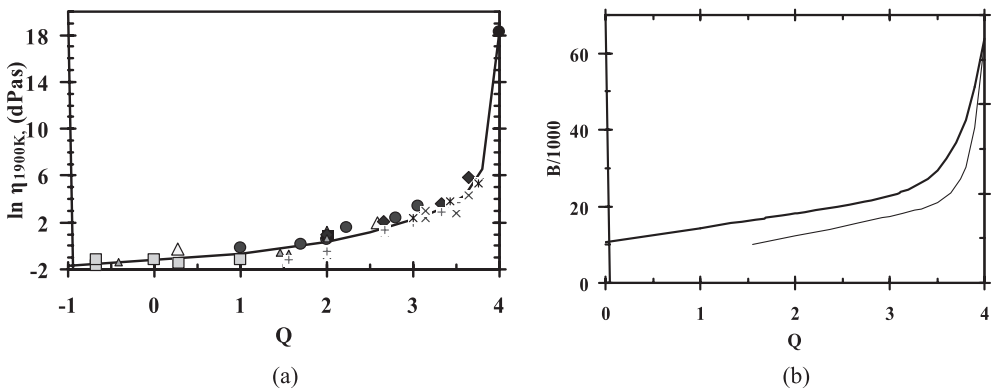

Fig. 2. (a) Viscosity ($\ln \eta_{l\,900\,K}$) and (b) the parameter, B_η, as functions of Q; note the upper curve in (b) is for MO-silicates and the lower curve is for M_2O-silicates.[7]

cations (with viscosity increasing with increasing cation size or decreasing field strength (z/r^2)).

The introduction of Al^{3+} into the Si^{4+} structure for slags with $Q>2.8$ results in a small linear increase in viscosity with increasing Q for alumina-silicates, in contrast with the dramatic increase in viscosity with increasing Q for silicates shown in Fig. 2(a).

Viscosity measurements on mould slags have been reported by several workers.[20–25] Experimental uncertainties can be up to 25%; McCauley[21] cites six sets of viscosity measurements on the same slag and the reported viscosities were found to vary by ±25%. Another source of uncertainty is that few workers cite chemical analysis on the post-measurement sample and fluorine and sodium losses can be significant during the experiment.

The new model to calculate the viscosities of mould slags is based on an earlier model proposed for slags in general[7] but which has required certain modifications in applying it to mould slags. In the original model, $\ln(\eta_{1\,900\ K})$ and the activation energy term, B_η, are represented as functions of Q as double exponential relations (Fig. 2). The small deviations from the curve due to cation effects can be accommodated in terms of the field strength for the cations (*i.e.* mean z/r^2).The activation energy term, B_η can also represented as a function of Q by two different double- exponential equations for MO-silicates and M_2O-silicates (Fig. 2(b) and Eqs. (28) and (29)). In mould slags, the charge balancing duties are carried out by K^+ and Na^+ ions, and this coupled with the fact that $X_{MO}>>X_{M2O}$ implies that the upper curve in Fig. 2(b) and Eq. (28) is more appropriate for casting slags. The viscosities at temperatures other than the reference temperature can be calculated from the Eq. (30).

$$\mathrm{MO-silicates:}\ B_\eta = 795\,830.8 + 8.476 \times 10^{-6}\exp(Q/0.2611) + 795\,841.4\exp(Q/211\,587.4) \quad \text{..... (28)}$$

$$\mathrm{M_2O-silicates:}\ B_\eta = -24.6 + 6.122 \times 10^{-13}\exp(Q/0.1258) + 28.465\exp(Q/7.727) \quad \text{... (29)}$$

$$\ln\eta_T = \ln\eta_{1\,900} + (B_\eta/T) - (B_\eta/1\,900) \quad \text{..... (30)}$$

The above model must be modified to apply it to mould slags since:

(i) the reference temperature, 1 573 K, is far removed from 1 900 K; this would have little effect on B_η but would have a dramatic effect on the ln η term since viscosity is sensitive to temperature changes.

(ii) both B_η and $\ln\eta_{1\,573\ K}$ are affected by both Q and the CaF_2 content, simultaneously.

Consequently, it is necessary to separate the effects of CaF_2 and Q. In the case of B_η (little affected by temperature) a value for a CaF_2-free slag can be obtained from Eq. (28); this is denoted as a solid curve in **Fig. 3**(a). It can be seen that B_η (i) increases with increasing Q and (ii) departs from the curve with deviations increasing with increasing CaF_2.Since B_η is dependent upon two factors (Q and X_{CaF2}), the various slags were then sorted into individual groups according to their X_{CaF2} values (*e.g.* (0–0.05); (0.05–0.1); *etc.*) and allocated a mean X_{CaF2} value (*e.g.* 0.025; 0.075, respectively). The departure of experimental values ($B_{\eta\ expt}$) from the curve (*i.e.* from Eq. (28), calculated using the remaining slag composition, $B_{\eta\ rem}$ Eq. (28)) is denoted ΔB_η, (defined in Eq. (31)) and was then plotted as a function of X_{CaF2} for specific groups of similar Q (*e.g.*{1.5±0.25}; {2±0.25} *etc.*); the results are shown in Fig. 3(b).

$$\Delta B_\eta = B_{\eta\ rem\ Eq\ 28} - B_{\eta\ expt} \quad \text{..... (31)}$$

$$B_\eta = (B_{\eta rem\ Eq\ 28} - \Delta B_\eta) = B_{\eta rem\ Eq\ 28} - 32.7X_{CaF2} \quad \text{..... (32)}$$

The same approach can not be adopted to treat the ln $\eta_{1\,573\ K}$ data because of the large differences in ln η values for 1 900 K and 1 573 K. Consequently, it is difficult to calculate a value of ln $\eta_{1\,573,\ CaF2}=0$ for CaF_2-free slags, since both Q and X_{CaF2} affect the viscosity simultaneously. The experimental data were first sorted into the same groups of similar X_{CaF2} values and these values were then plotted as function of Q (**Fig. 4**(a)) and equations were derived for ln $\eta_{1\,573\ K}$ as a function of Q. A linear best fit of the data ($\ln\eta_{1\,573\ K}=3.073+1.93Q$) was then derived since the relationship is close to linear in the range $Q=1.5$ to 3.Then the database was divided into groups of similar Q values and plotted against the mole fraction of CaF_2 (Fig. 4(b)). The mean gradient of these plots ($d\ln\eta_{1\,573}/dX_{CaF2}$)=−9 was determined from these plots. Values of ln $\eta_{1\,573,\ CaF2=0}$ were then calculated using Eq. (33); the values of ln $\eta_{1\,573,\ CaF2=0}$ were then plotted against Q (**Fig. 5**) and the best fit curve for ln $\eta_{1\,573,\ CaF2=0}$ is given in Eq. (34). It can be seen that the mean scatter in ln $\eta_{1\,573}$ values is about 0.3.which corresponds to an uncertainty of *ca.* ±25% in η. Attempts will be made in the future to reduce this uncertainty from a best fit regression of ln $\eta_{1\,573}$ data as functions of Q and X_{CaF2}. The calculated viscosity values are compared with values calculated by the Riboud[26] and Iida models[27] in the Viscosity worksheet and mean values for the three models were also calculated.

$$\ln\eta_{1\,573,\ CaF2=0} = \ln_{\eta 1\,573} - 9X_{CaF2} \quad \text{..... (33)}$$

$$\ln\ \eta_{1\,573K,ref} = 0.1227\exp\ (1.1454\ Q) \quad \text{..... (34)}$$

Although viscosity measurements for supercooled liquids

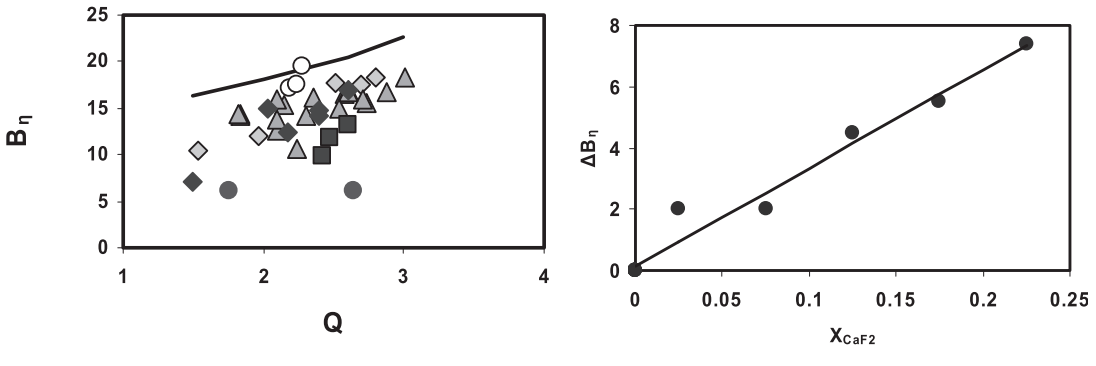

Fig. 3. (a) The parameter, B_η, as a function of Q for slags containing varying X_{CaF2}: for following X_{CaF2} ranges: line = 0; o = 0–0. 05; ◊ = 0.05–0.1; Δ = 0.1–0.15; ♦ = 0.15–0.2; ■ = 0.2–0.25; ● = >0.25 and (b) ΔB_η as a function of X_{CaF2}.

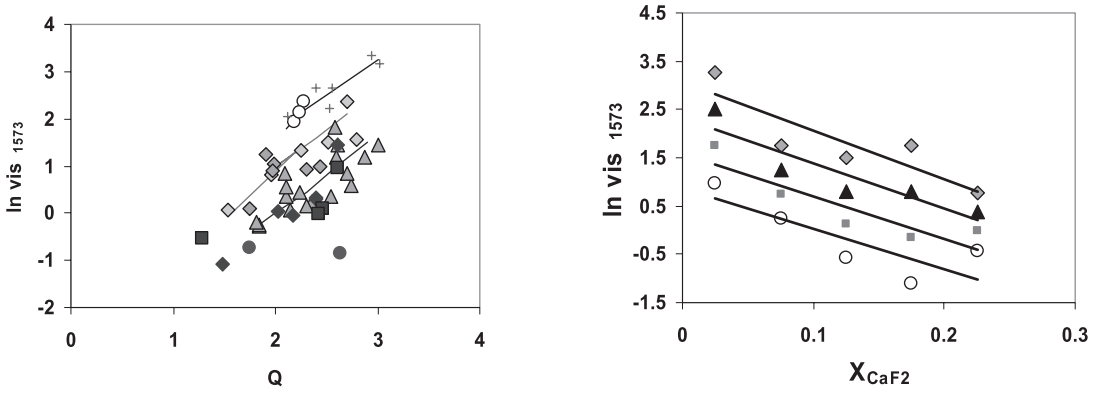

Fig. 4. The parameter, ln $\eta_{l\ 573\ K}$ as functions of (a) Q; X_{CaF2}=(0.025±0.025)=O,+; black line (0.075±0.025)=♦ and red line,; (0.125±0.025)=▲ and green line;(0.175±0.025)=♦; (0.225 ±0.025)=■; >0.25=● and (b) mole fraction CaF_2; O=(Q=1.5); ■=(Q=2); ▲=(Q=2.5); ♦=(Q=3).

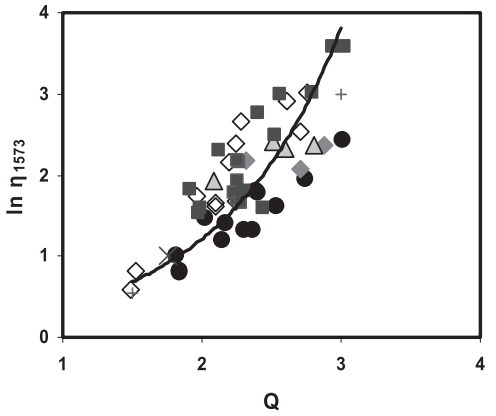

Fig. 5. Values of ln $\eta_{l573,\ CaF2=0}$ for various mould slags as a function of the parameter Q; ◊=Lanyi;[20] ■, x=McCauley[21] ●=Persson[22] ♦ Elahipanah.[23]

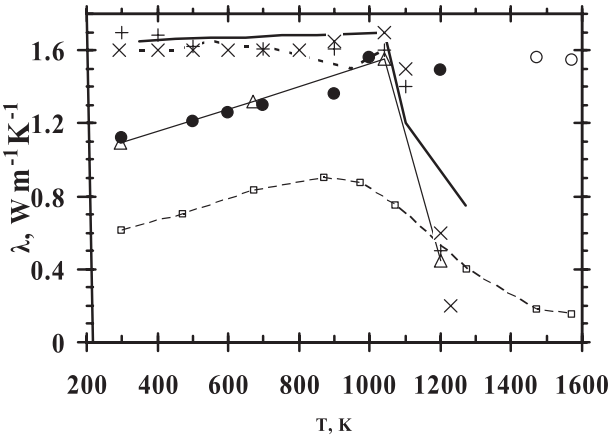

Fig. 6. Thermal conductivity of mould slags as a function of temperature; Glassy phase:=faint line=k_{THW}[7] and ●,○ k_{LP} values for solid and liquid calculated from 10^7a=4.5 and 4 m^2s^{-1},respectively;[16,18,28–31] partially- crystalline slags=X, + and dashed, bold line and bold line: Δ,□=partially-melted powders[32] values recorded on cooling after melting.

are available for minerals and glasses, measurements on slags are rare for metallurgical slags and the authors were unable to obtain any experimental data for the *scl* state of mould slags. However, it is possible to calculate values for these slags in the *scl* range since $\log_{10}\ \eta$ (d Pas) has values of 13.4 and 6, respectively, at T_g and T_{crit} (=1 040 ±10 K). These data can be coupled with calculated values for the liquid range at T_{liq}, 1 573 and 1 673 K. Attempts were made to obtain a best fit for these data using a polynomial relation ($\log_{10}\ \eta$(d Pas)=a+bT+cT^2+dT^3 where a, b, c and d are constants). Unfortunately, the resulting value for $\log_{10}\ \eta$ at T_g departed significantly from $\log_{10}\ \eta$ (dPas)=13.4 in some cases. Consequently, values of $\log_{10}\ \eta$ (d Pas) were obtained from linear relationships between T_g and T_{crit} and between T_{crit} and T_{liq}; these values should not be regarded as accurate values for the *scl* but do provide the reader with approximate values which are unavailable in the literature.

The performance of the new model was tested by calculating the viscosity at 1 573 K and comparing it with the experimental values for *ca*. 30 mould powders.[20–25] The slags were randomly selected to give a range of $\eta_{l\ 573}$ values (0.5–12 dPas) but slags containing >1% B_2O_3, >1% ZrO_2 and >3%FeO were excluded. The deviation (Δ=100 (η_{calc}-η_{exp})/η_{exp}) was calculated and the mean deviation determined (Δ_{mean}=[Δ_1^2+ Δ_2^2+ Δ_3^2+...]$^{0.5}$). Then the Δ_{mean} values were compared with those for the Riboud[26] and Iida[27] models. It was found that performances of the new model, the Riboud and Iida models were similar (Δ_{mean}=35%; 35% and 43%, respectively). It was found that the mean $\eta_{l\ 573}$ value for the three studies was closer to the experimental values (Δ_{mean}=27%). It should be noted the experimental uncertainties associated with both the viscosity measurements and changes in chemical composition during the measurement sequence are *ca*. ±25% for most of the reported data.

2.6. Thermal Conductivity (k) and Thermal Diffusivity (a)

The thermal conductivity of the slag film is important in controlling the heat transfer from the shell. Thermal conductivities of liquid slags are difficult to measure since it is difficult to eliminate contributions from convection. This is usually achieved by using transient methods where the experiment is completed before convection is initiated. The two principal, transient techniques are the laser pulse (LP) and the Transient Hot wire (THW) methods.

However, glassy and liquid slags are also semi-transparent to infra-red radiation and heat transfer can occur simultaneously by both lattice conductivity (k_{lat}) and radiation conductivity (k_R).Most investigators try to determine the values of k_{lat} and k_R, individually and then combine them to give a total value. However, recent measurements of k_{lat} on mould slags using the LP and THW methods reveal that: (i) Values of k_{LP}[16,18,28–31] and k_{THW}[8,9,35–37] are in good

agreement up to 1 000 K (Fig. 6) but deviate markedly at higher temperatures.

(ii) The k_{THW} values for mould slags drop markedly for temperatures >1 040 K, in contrast to k_{LP} values which continue to rise (Fig. 6); this contradictory behaviour has been attributed variously, to electrical leakage in the THW measurements or to k_R contributions to k_{LP} in the LP measurements.

The source of the discrepancy between k_{LP} and k_{THW} is unresolved at the present time. Here it has been assumed that k_{LP} measurements contain contributions from k_R and the k_{THW} measurements have been adopted.

The thermal conductivities of slags are also affected by (i) the *degree of crystallinity* developed in the slag (*i.e.* f_{crys}) since $k_{crys} \approx 2\ k_{glass}$ due to the higher packing density in the crystalline phase than in the glass and (ii) *porosity* which tends to reduce the thermal conductivity. Note crystallisation is accompanied by shrinkage and results in the formation of fine pores in slag films.

Plots of k_{THW} for ***glassy***, M_2O–CaO–SiO_2 slags versus the calculated viscosities indicated that the sharp drop in k_{THW} occurred at the temperature where $\eta = 10^6$ d Pas;[7,13] thus T_{crit} occurs midway between the *softening* temperature (where the sample can no longer support its own weight) and the *flow temperature*.[7,13] The collapse in k_{THW} occurs for the *scl* phase (*i.e.* in glassy samples). This strongly suggests that the magnitude of the thermal conductivity is linked to the rigidity of the silicate lattice.[7,13] Measured k_{THW} values ranged from 1.05–1.09 $Wm^{-1}K^{-1}$ at 298 K for glass samples;[8,9] so a value of $k_{298} = 1.07 \pm 0.02$ $Wm^{-1}K^{-1}$ was adopted for all glassy mould fluxes.

The following values were also reported for the glassy phase, $T_{crit} = 1\ 040 \pm 10$ K and $k_{Tcrit} = 1.65 \pm 0.05$ $Wm^{-1}K^{-1}$.[7] Measurements of k_{THW} for 15 mould slags indicated that $k_{1\ 040\ K} = 1.65 \pm 0.05$ $Wm^{-1}K^{-1}$;[8,9] thus k_T values between 295 K and 1 040 K can be calculated using Eq. (35). Note that if $k_{295} > 1.65$ $Wm^{-1}K^{-1}$ the temperature coefficient (dk/dT) will be negative and if $k_{295} < 1.65$ $Wm^{-1}K^{-1}$, (dk/dT) will be positive

$$(295 - 1\ 040\ \mathrm{K}):\quad k_T\left(Wm^{-1}K^{-1}\right) = 1.07 + 0.00078\ (T - 295K) \quad \ldots\ldots (35)$$

A large number of thermal diffusivity (a_{LP}) values for casting slags in the glassy, crystalline and liquid states have been measured[16,28–31] with the LP method; values of k_{LP} were derived using Eq. (36).

$$k_{LP} = a_{LP} . / \rho\ C_p \quad \ldots\ldots (36)$$

The model determines the thermal conductivity at three temperatures, namely, 298 K, T_{crit} (=1 040 K) and T_{liq}; the k-T curves between (298 K and T_{crit}) and also (T_{crit} and T_{liq}) are assumed to be linear. There are insufficient data available for the temperature coefficient (dk/dT) of the liquid slag at the present time to permit calculation of values for liquid mould slags.

The ***super-cooled liquid*** phase is formed at temperatures above T_g (> *ca.* 870 K) but the sharp drop in k_{THW} does not occur until the temperature exceeds the critical (or deformation) temperature, T_{crit}. Values of k_T between T_{crit} and T_{liq} are calculated using Eq. (37).

$$(1\ 040\ \mathrm{K} - T_{liq}):\quad k_T\left(Wm^{-1}K^{-1}\right) = 1.65 - \left\{\left(1.65 - k_{Tliq}\right)\left(T_{liq} - T\right)\right\} / \left(T_{liq} - 1\ 040\ \mathrm{K}\right) \quad \ldots\ldots (37)$$

In ***partially-crystalline*** slags (or slag films) the thermal conductivity increases with increasing crystallinity[8,28,30,33] since ($k_{cryst} \approx 2\ k_{glass}$). Values of k_{295} for partially-crystalline slags are calculated from Eq. (38)[8,9] using the f_{cryst} derived with Eq. (7). It should be noted that Eq. (38) may produce a slightly low k_{295} value for a 100% crystalline slag (*i.e.* $k \approx 2$ $Wm^{-1}K^{-1}$) since crystallisation is accompanied by porosity, which lowers the conductivity of the sample. A fully crystalline sample would not be expected to show the collapse in k_T above T_{crit} exhibited by glasses (Fig. 6); thermal diffusivity values for a fully crystalline sample appear to remain reasonably constant with increasing temperature above 1 040 K. Thus, k_T has been assumed to remain constant for crystalline samples until the sample melts. However, slag films with a reasonable amount of glassy phase would be expected to show some collapse in k_T above T_{crit}.

$$k_{295}\left(Wm^{-1}K^{-1}\right) = 1.07 + 0.7\ f_{cryst} \quad \ldots\ldots (38)$$

When the glass is heated above *ca.* 1 000 K, crystallisation of the sample occurs; note crystallisation occurs roughly in the same temperature range as T_{crit}; the model takes no account of any subsequent change in f_{crys}. Values of k_T for partially-crystalline samples in the temperature range (1 040 K -T_{liq}) are calculated using Eq (37).

There are few measurements of the thermal conductivity of ***liquid mould slags*** using the k_{THW} method,[8,32,34] but several workers[18,28–31] have reported values for the thermal diffusivity of liquid mould slags ($a_{LP} = 4 \times 10^{-7}$ m^2s^{-1}) using the LP method which yields values for k_{LP} which are about 10 x higher than k_{THW} values (Fig. 6). The k_{THW} values have been tentatively, adopted. Eq. (39) was obtained from a relation reported for slags covering a wide compositional range.[7]

$$k^m{}_{THW}\left(liq\right) = 0.139 + 3.65 \times 10^{-5} \exp\left(Q / 0.3421\right) \quad \ldots\ldots (39)$$

Values of k_{298} have been reported for slag films taken from the mould.[9,12] Approximate values for k_{295} of the slag film can be calculated by using Eq. (40) where f_{cryst} is calculated from Eq. (7). Note $k_{298} = \mathbf{1.77}$ $Wm^{-1}K^{-1}$ is calculated with Eq. (38) for $f_{crys} = 1$ and refers to a sample containing pores.

$$k_{298}\left(\text{slag film}\right) = 1.77\ f_{crys} + 1.07\left(1 - f_{crys}\right) Wm^{-1}K^{-1} \quad \ldots\ldots (40)$$

There are two outstanding problems to be resolved concerning thermal conductivity measurements, namely (i) the differences between k_{THW} and k_{LP} for temperatures above 1 040 K and (ii) the degree of porosity in slag film and partially-crystalline samples which has not yet been determined and which makes it difficult to determine the k value for a fully-dense slag. The calculated thermal conductivity values of the glass and partially-crystalline phases are probably prone to uncertainties of *ca.* ±5% and ±10%, respectively, for temperatures between 298 and 1 040 K. However for temperatures >1 040 K, it is difficult to attribute uncertainties until the differences between k_{THW} and k_{LP} are fully explained.

2.7. Surface Tension (γ) and Interfacial Tension (γ_{msl})

Surface tension is a surface property and not a bulk property. The magnitude of the surface tension is determined by the composition of the surface. Components with low surface tension (denoted *surfactants*) tend to occupy the surface layer and hence largely determine the surface tension. Components such as CaO, MgO and Al_2O_3 have high surface tensions (**Table 3**) compared with the surface tension of SiO_2 and the surfactants (B_2O_3, K_2O, Na_2O and CaF_2).

The temperature dependence of surface tension ($d\gamma/dT$) is usually negative for most components but as the concentration of surfactants increases ($d\gamma/dT$) becomes less negative

Table 3. Values for slag components of surface tension (γ, mNm^{-1}), temperature coefficient ($d\gamma/dT$, mNm^{-2})[41] and Gibbs energy of formation for liquid oxides per O atom ($-\Delta G_i$)[43] used to calculate interaction parameter, φ.[42] The last row provides equations used to calculate depression of surface tension ($X_i\gamma_i$) by surfactants.[41]

	SiO_2	CaO	Al_2O_3	MgO	Na_2O	K_2O	Li_2O	FeO	MnO	CaF_2	ZrO_2	TiO_2	B_2O_3
$\gamma_{1\,773}$	260	625	655	635	297	160	[300]	645	530	290	400	350	110
$d\gamma/dT$	0.031	−0.094	−0.177	−0.13	−0.11	−0.11	−0.11	−0.1	−0.1	−0.07	−0.15	−0.15	
$-\Delta G_i$ $kJmol^{-1}$	292.2	408.2	354.6	368.4	195.2	140	357	158	240.5	466	365	304	
Surfactant			Na_2O			K_2O			CaF_2			B_2O_3	
Equation $(X_i\gamma_i)^{surf}$			$=-0.8-1\,388\,X_i^{surf}$ $+6\,723\,(X_i^{surf})^2$			$=-0.8-1\,388\,X_i^{surf}$ $+6\,723\,(X_i^{surf})^2$			$=-2.934\,X_i^{surf}$ $+4\,769\,(X_i^{surf})^2$			$=-5.2-3.454\,X_i^{surf}$ $+22\,178(X_i^{surf})^2$	

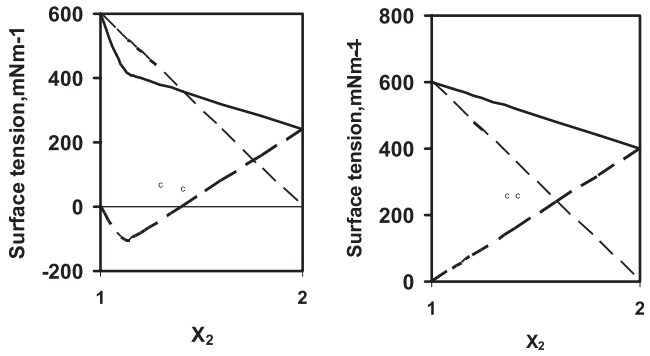

Fig. 7. Schematic diagram showing compositional dependence (X) of surface tension (γ=solid line) and X_1 γ_1 and X_2 γ_2 (=dashed lines) for a binary slag system containing (a) no surface active constituents and (b) one bulk constituent (1) and one surfactant (2).[41]

and eventually changes to a positive value.

Few surface tension measurements have been reported for mould slags.[17,18,35–40] The model is based on a previous model[41] in which the following assumptions were made:

(i) The various slag components were divided into, *surfactants* and *bulk components*.

(ii) The surface tension of bulk components (**Fig. 7**(a)) at 1 773 K were calculated using partial molar values for the various components $(\gamma=X_1\gamma_1+X_2\gamma_2+X_3\gamma_3)^{bulk}$.

(iii) It was found that $X_i\gamma_i$ contributions for surfactants resulted in a sharp drop in surface tension until a certain point was achieved (in the range, $X_i=0.1$ to 0.12) and the relation (up to this point) is expressed as, $(X_1\gamma_1=a'+b'X_1+c'X_1^2)$. Above this point, γ increased gradually (Fig. 7(b)) with increasing X (in range, 0.12 to 1.0 and is expressed as $(X_1\gamma_1=d'+e'X_1)$.

When this model was applied to mould slags (which contain a reasonably high concentration of surfactants) it was found that it tended to produce low values for the surface tension.[41]

Consequently, the model was modified and the following assumptions were made:

(i) That the minimum in the surfactant curve in Fig. 7(b) corresponded to the point where the slag surface was saturated with surfactants ($X_{surf}=0.12$).

(ii) That the surface is occupied preferentially by $B_2O_3>K_2O>Na_2O>CaF_2$ until the surface becomes saturated with surfactant at $\Sigma X_{surf}=0.12$; $(X_i\gamma_i)^{surf}$ is calculated using the values for surfactants given in Table 3.

(iii) Any excess surfactant (left after $\Sigma X_{surf}=0.12$) is treated as a bulk component $(\gamma=X_1^{xs}\gamma_1+X_2^{xs}\gamma_2)$.

(iv) The temperature dependence ($d\gamma/dT$) was calculated from Eq. (41).

$$(d\gamma/dT)=[X_1(d\gamma_1/dT)+X_2(d\gamma_2/dT)] \quad \text{..... (41)}$$

The surface tension is then calculated from Eqs. (42) and (43)

$$\gamma_{1\,773K}=[(X_1\gamma_1+X_2\gamma_2+X_3\gamma_3)^{conv}+(X_1^{xs}\gamma_1+X_2^{xs}\gamma_2)+\Sigma(X_i\gamma_i)^{surf}] \quad \text{..... (42)}$$

$$\gamma_T=\gamma_{1\,773K}+(d\gamma/dT)(T-1\,773) \quad \text{..... (43)}$$

There is a limited amount of data to test the predictions and the reported data show significant variation. Nevertheless, the calculated values are in good agreement with the measured values.[1,18,35–40] The uncertainty associated with the estimations is probably *ca.* ±10%.

The ***interfacial tension*** **(γ_{msl})** can be calculated from Eq. (44) where γ_m=steel surface tension, γ_{sl} can be derived from Eqs. (42) and (43) and the interaction coefficient, φ, can be calculated using Eqs. (45) and (46), where ΔG_i is the free energy of formation of the individual, liquid oxides[42,43] with the values being given in Table 3.[43] Thus, φ is treated as a measure of the oxide components in the slag to supply soluble oxygen in the metal and thereby, decrease the interfacial tension, γ_{msl}. The value of γ_{msl} is largely determined by γ_m since $\gamma_m\approx$ (4 to 5) γ_{sl} and the value of γ_m, in turn, is largely determined by the S content of the steel. The calculated values of γ_{msl} obtained with this procedure were reported to lie within ±100 mNm^{-1} of the experimental values.[42] Values of γ_{msl} are calculated in steel property estimation software, worksheet "surface tension".

$$\gamma_{msl}=\gamma_m+\gamma_{sl}-2\varphi(\gamma_m\gamma_{sl})^{0.5}. \quad \text{..... (44)}$$

$$\varphi=0.89-1.5\times10^{-3}\Delta G_i^D. \quad \text{..... (45)}$$

$$\Delta G_i^D.==\Delta G_{FeO}-\Sigma\, X_i\Delta G_i. \quad \text{..... (46)}$$

2.8. Emissivity (ε_{TN})

Total normal emissivity measurements have been reported for mould slags;[6] values were recorded for the solid (at T>1 030 K) $\varepsilon_{TN}=0.92\pm0.05$ and liquid, $\varepsilon_{TN}=0.91\pm0.03$.

3. Results and Discussion

Routines have been developed in this study to calculate the following properties of mould slags from their chemical composition for subsequent use as input data in mathematical models of the continuous casting process: T_{liq}, T_g, T_{br}; T_{crit}; C_p (H_T-H_{298}); density and α; viscosity, thermal conductivity, surface and interfacial tension and emissivity.

Although mould slags have relatively low melting points and are benign in their behaviour, there are few measure-

ments available for some properties (*e.g.* C_p, enthalpy, density and surface tension). By contrast, there are a large number of reported data for viscosity and for thermal conductivity/diffusivity. However, there is high level of experimental uncertainty with viscosity measurements (±10–25%) and there is an unresolved dispute regarding the thermal conductivity values at temperatures at >1 040 K derived using the THW and LP methods. It is important that this dispute be settled quickly. One further problem is that many workers fail to report post-measurement analysis of their samples and F and Na losses can be significant during a measurement campaign and affect the property values. This study aims to provide reliable property data for the mould slag for use in mathematical models of continuous casting. Consequently, it is intended to update the existing software as new data become available. The following improvements in the software are planned:

(i) The present software does not include B_2O_3 additions since various workers report B_2O_3 causes both increases and decreases in slag viscosity.
(ii) To include calcium-aluminate- based slags used for casting high Al steels.
(iii) To improve the viscosity model for the super-cooled liquid phase.

4. Conclusions

(1) Routines have been developed to calculate the thermo-physical properties of mould slags from their chemical composition for their subsequent use in mathematical models of heat and fluid flow in the continuous casting mould.

(2) The accuracies of estimated values are affected by the limitations in the experimental data.

(3) The cause of the huge discrepancies in thermal conductivities for T>1 050 K must be resolved.

Acknowledgements

This work was made possible by the facilities and support provided by the EU (RFSR-PR-10005 DDT), the Research Complex at Harwell, and the EPSRC (EP/I02249X/1).

Symbols Abbreviations

a = Thermal diffusivity (m^2s^{-1})
C_p = Heat capacity ($JK^{-1}mol^{-1}$ or $JK^{-1}kg^{-1}$)
f_{cryst} = Fraction crystalline phase
f^* = Fraction of powder forming slag
(H_T-H_{298}) = Enthalpy relative to 298 K ($Jmol^{-1}$ or Jkg^{-1})
k = Thermal conductivity ($Wm^{-1}K^{-1}$)
S = Entropy ($JK^{-1}kg^{-1}$)
T = temperature (K)
X = Mole fraction
α = Thermal expansion coefficient(K^{-1})
γ = Surface tension (mNm^{-1})
γ_{ms} = Interfacial tension (mNm^{-1})
η = Viscosity (dPas)
ρ = Density (kgm^{-3})
BO = Bridging Oxygens
FO = Free Oxygens
LP = Laser pulse method
NBO = Non-bridging Oxygens
NBO/T = Measure of de-polymerisation
THW = transient hot wire method
Q = measure of polymerisation
scl = super-cooled liquid

Subscripts and Supercripts

^{m} = Value for liquid at T_{liq}.

REFERENCES

1) P. Ramirez-Lopez, K. C. Mills, P. D. Lee and B. Santillana: *ISIJ Int.*, **50** (2010), 1797.
2) Y. Meng, B. G. Thomas, A. A. Polycarpou, A. Prasad and H. Henein: *Can. Metall. Q.*, **45** (2006), 79.
3) P. Ramirez-Lopez, K. C. Mills, P. D. Lee and B. Santillana: *Metall. Mater. Trans. B*, **43B** (2012), 109.
4) J. F. Stebbins: Chapter in Encyclopedia of Glass Technology ed. by P. Richet, Wiley, New York, (2016), in press.
5) Z. Li, R. Thackray and K. C. Mills: 7th Int. Conf. Molten Slags, Fluxes and Salts, SAIMM, Johannesburg, South Africa, (2004), 813.
6) K. C. Mills, A. Olusanya, R. Brooks, R. Morrell and S. Bagha: *Ironmaking Steelmaking*, **15** (1988), 257.
7) K. C. Mills, L. Yuan, Z. Li and G. H. Zhang: *High Temp.-High Press.*, **42** (2013), 237.
8) P. Andersson: *Ironmaking Steelmaking*, **42** (2015), 456, 465.
9) P. Andersson: *Ironmaking Steelmaking*, (2016), in press.
10) S. Sridhar, K. C. Mills, O. D. C. Afrange, H. P. Lorz and R. Carli: *Ironmaking Steelmaking*, **27** (2000), 238.
11) K. C. Mills and B. J. Keene: *Int. Mater. Rev*, **22** (1987), 1.
12) M. Susa, K. C. Mills, M. J. Richardson, R. Taylor and D. Steward: *Ironmaking Steelmaking*, **21** (1994), 279.
13) K. C. Mills, L. Yuan, Z. Li, G. H. Zhang and K. C. Chou: *High Temp. Mater. Process.*, **31** (2012), 301.
14) L. Courtney, S. Nuortie-Perkio, C. A. G. Valadares, M. J. Richardson and K. C. Mills: *Ironmaking Steelmaking*, **28** (2001), 412.
15) R. Olivares, M. P. Brungs and H. Liang: *Metall. Mater. Trans. B*, **22B** (1991), 305.
16) R. Taylor and K. C. Mills: *Ironmaking Steelmaking*, **15** (1988), 187.
17) T. Matsushita, T. Ishikawa, P. F. Paradis, K. Mukai and S. Seetharaman: *ISIJ Int.*, **46** (2006), 606.
18) B. J. Monaghan and R. F. Brooks: *Ironmaking Steelmaking*, **29** (2002), 115.
19) J. F. Stebbins, I. S. E. Carmichael and I. K. Moret: *Contrib. Mineral. Petr.*, **86** (1984), 131.
20) M. Lanyi and C. F. Rosa: *Metall. Mater. Trans. B*, **12B** (1981), 287.
21) W. McCauley and D. Apelian: *Can. Metall. Q.*, **20** (1981), 247.
22) M. Persson, M. Gonerup and S. Seetharaman: *ISIJ Int.*, **47** (2007), 1540.
23) Z. Elahipanah: MSc Thesis, KTH, Stockholm, (2012), available on line, www.diva-portal.se/smash/get/diva2:547031/FULLTEXT01.pdf, (accessed 2014-01-01).
24) J. W. Kim, J. Choi, O. D. Kwon, I. R. Lee, Y. K. Shin and J. S. Park: 4th Int. Conf. Molten Slags and Fluxes, ISIJ, Tokyo, (1992), 468.
25) K. C. Mills, L. Chapman, A. B. Fox and S. Sridhar: *Scand. J. Metall.*, **30** (2001), 396.
26) P. V. Riboud, Y. Roux, L. D. Lucas and H. Gaye: *Fachber. Huttenprax. Metallweiterv.*, **19** (1981), 859.
27) T. Iida, H. Sakai, Y. Kita and K. Murakami: *High Temp. Mater. Process.*, **19** (2000), 153.
28) H. Shibata, J. W. Cho, T. Emi and M. Suzuki: 5th Int. Conf. Molten Slags, Fluxes and Salts, ISS, Warrendale, PA, (1997), 771.
29) M. Gonerup, M. Hayashi, C. A. Dacker and S. Seetharaman: 7th Int. Conf. Molten Slags, Fluxes and Salts, SAIMM, Johannesburg, South Africa, (2004), 745.
30) M. Hayashi, A. A. Riad and S. Seetharaman: *ISIJ Int.*, **44** (2004), 691.
31) H. Ohta, M. Masuda, K. Watanabe, K. Nakajima, H. Shibata and Y. Waseda: *Tetsu-to-Hagané*, **80** (1994), 463.
32) K. Nagata and K. S. Goto: 2nd Int. Conf. Metall. Slags and Fluxes, ed. by H. A. Fine and D. R. Gaskell, TMS-AIME, Warrendale, PA, (1984), 875.
33) S. Ozawa, M. Susa, T. Goto, H. Kojima and K. C. Mills: *ISIJ Int.*, **46** (2006), 413.
34) J. S. Powell: Unpublished data, cited in Ref. 16).
35) Y. Lu, G. D. Zhang and M. F. Jiang: *Adv. Mater. Res.*, **233–235** (2011), 805.
36) Y. Lu, X. Fang and G. D. Zhang: *Adv. Mater. Res.*, **287–290** (2011), 1866.
37) Y. Lu, G. D. Zhang and X. Yu: *Appl. Mech. and Mater.* **71–78** (2011), 2899.
38) Y. Lu, X. Fang and X. Yu: *Adv. Mater. Res.*, **455–456** (2012), 134.
39) Y. Lu and G. D. Zhang: *Mater. Sci. Forum.*, **675–677** (2011), 877.
40) H. Y. Cheng, Y. Wang, D. Li and M. Hu: *Contin. Cast.*, (2008), No. 4, 42.
41) K. C. Mills: Am. Chem, Soc Symp. Series 301, Mineral Matter and Ash in Coal, ed. by K. S. Vorres, Am. Chem. Soc., Washington, DC, (1986), 195.
42) Y. Chung and A. W. Cramb: *Metall. Mater. Trans. B*, **31B** (2000), 957.
43) Y. Chung: PhD Thesis Carnegie-Mellon University, Pittsburgh, PA, (1999), 179.